JBC ARTICLE

Carnosine synthase deficiency is compatible with normal skeletal muscle and olfactory function but causes reduced olfactory sensitivity in aging mice

Received for publication, May 2, 2020, and in revised form, October 7, 2020 Published, Papers in Press, October 9, 2020, DOI 10.1074/jbc.RA120.014188

Lihua Wang-Eckhardt[1], Asisa Bastian[1], Tobias Bruegmann[2], Philipp Sasse[2], and Matthias Eckhardt[1,*]

From the [1]Institute of Biochemistry and Molecular Biology, Medical Faculty and [2]Institute of Physiology I, Medical Faculty, University of Bonn, Bonn, Germany

Edited by Paul E. Fraser

Carnosine (β-alanyl-L-histidine) and anserine (β-alanyl-3-methyl-L-histidine) are abundant peptides in the nervous system and skeletal muscle of many vertebrates. Many *in vitro* and *in vivo* studies demonstrated that exogenously added carnosine can improve muscle contraction, has antioxidant activity, and can quench various reactive aldehydes. Some of these functions likely contribute to the proposed anti-aging activity of carnosine. However, the physiological role of carnosine and related histidine-containing dipeptides (HCDs) is not clear. In this study, we generated a mouse line deficient in carnosine synthase (Carns1). HCDs were undetectable in the primary olfactory system and skeletal muscle of Carns1-deficient mice. Skeletal muscle contraction in these mice, however, was unaltered, and there was no evidence for reduced pH-buffering capacity in the skeletal muscle. Olfactory tests did not reveal any deterioration in 8-month-old mice lacking carnosine. In contrast, aging (18–24-month-old) Carns1-deficient mice exhibited olfactory sensitivity impairments that correlated with an age-dependent reduction in the number of olfactory receptor neurons. Whereas we found no evidence for elevated levels of lipoxidation and glycation end products in the primary olfactory system, protein carbonylation was increased in the olfactory bulb of aged Carns1-deficient mice. Taken together, these results suggest that carnosine in the olfactory system is not essential for information processing in the olfactory signaling pathway but does have a role in the long-term protection of olfactory receptor neurons, possibly through its antioxidant activity.

Carnosine (β-alanyl-L-histidine), the first peptide ever isolated from an animal tissue (1), and related peptides (histidine-containing dipeptides (HCDs)) are present at exceptional high (millimolar) concentrations in skeletal muscle and the primary olfactory system (2, 3) (see Boldyrev *et al.* (4) for a comprehensive review). HCDs are also present in various other tissues although at significantly lower concentrations (4, 5). Carnosine is synthesized by a cytosolic amino acid ligase, carnosine synthase (Carns1; also known as ATP-grasp domain–containing protein 1, ATPGD1; EC 6.3.2.11) (6). In the presence of GABA (*i.e.* in the central nervous system), Carns1 also catalyzes the synthesis of homocarnosine (γ-aminobutyryl-L-histidine). Carnosine can be modified by *N*-methyltransferases (7, 8) in a tissue- and species-specific manner, forming ophidine (β-alanyl-1-methyl-L-histidine) or anserine (β-alanyl-3-methyl-L-histidine). The latter is the most abundant HCD in skeletal muscle of mice, rats, and other rodents (4). The highest concentrations of HCDs (>10 g/kg, *i.e.* >40 mM) have been found in muscles from several birds, especially some Galliformes families, some teleostei (*e.g.* marlin) (mainly anserine), and cetacea species (mainly ophidine) (4). Carnosine and anserine are degraded by serum carnosinase 1 (EC 3.4.13.20) (9). A homologous enzyme, cytosolic nonspecific dipeptidase or carnosinase 2 (EC 3.4.13.18), exhibiting a much broader substrate specificity also hydrolyzes anserine and carnosine *in vitro*, but it is not clear to what extent this enzyme is actually involved in carnosine turnover (10, 11).

In the olfactory system, carnosine is most likely exclusively synthesized in receptor neurons of the olfactory epithelium (OE) (12). Carnosine co-localizes with glutamate in the presynapse of synapses between olfactory receptor neurons and mitral cells (13), and its release from synaptosomes prepared from the olfactory bulb is calcium-dependent and stimulated by depolarization (14). It was therefore proposed that carnosine may act as neurotransmitter or neuromodulator in the primary olfactory system (15). In line with this, carnosine exhibits excitatory activity on mitral cells in the OB (16). In contrast, however, Harding and O'Fallon (17) did not find evidence for the presence of carnosine in synaptic vesicles. It was also proposed that carnosine (and homocarnosine) may be involved in neuron-to-glia signaling (18).

In contrast to the primary olfactory system, carnosine appears to be synthesized by glial cells in other parts of the nervous system (19). There mainly (if not exclusively) oligodendrocytes are responsible for its synthesis (20). The glutamate receptor activation–dependent release of carnosine from oligodendrocytes (21) suggests a possible role of the peptide in glia-neuron interaction (22). In heart and skeletal muscle, carnosine affects muscle function via improving pH buffering and/or excitation-contraction coupling by local calcium recruitment (23, 24). Besides these potential roles in neuron-glia signaling and muscle excitation-contraction coupling, other less specific functions of carnosine have been documented (4). Particularly, carnosine has antioxidative activity (25) and inhibits protein carbonylation and glycation as well as the formation of

* For correspondence: Matthias Eckhardt, eckhardt@uni-bonn.de.
Present address for Tobias Bruegmann: DZHK e.V. (German Center for Cardiovascular Research), Partner Site Goettingen, Goettingen, Germany; Institute for Cardiovascular Physiology, University Medical Center Goettingen, Goettingen, Germany.

advanced glycation end products (AGEs) and advanced lipoxidation end products (ALEs) (4). These processes are likely involved in the anti-aging activity of carnosine (26). Whether the beneficial effects of exogenously supplied carnosine, however, reflect the physiological function of the endogenously synthesized peptide is unclear. To be able to further explore the physiological role of HCDs, we generated Carns1-deficient (Carns1(−/−)) mice. We focused our analysis on the two tissues/systems with by far the highest HCD concentration: skeletal muscle and primary olfactory system. Aging Carns1(−/−) mice exhibited diminished olfactory sensitivity and loss of olfactory receptor neurons, suggesting a role of carnosine in long-term survival of olfactory receptor neurons (ORN).

Results

Carns1(−/−) mice lack carnosine and anserine

Mice deficient in Carns1 were generated by homologous recombination in HM-1 embryonic stem cells (Fig. 1). The targeting construct introduced loxP sites within intron 2 and in exon 10, resulting in deletion of the complete coding region of Carns1 after cre recombinase action (Fig. 1*A*). Correct targeting was confirmed by Southern blot analysis (Fig. 1*B*) and PCR (data not shown), and an embryonic stem (ES) cell clone showing homologous recombination in both alleles (*f/f* in Fig. 1*B*) was used for generating chimeric and subsequently Carns1 (−/−) mice. Absence of the Carns1 mRNA in Carns1(−/−) mice was confirmed by Northern blot analysis (Fig. 1*C*). Real-time RT-PCR showed ∼50% reduction in the expression of Carns1 in heterozygous mice (Fig. 1*D*). Western blot analysis using a newly generated Carns1 antiserum confirmed absence of the enzyme in Carns1(−/−) and reduced levels in heterozygous mice compared with WT littermates (Fig. 1*E*). As expected, carnosine and anserine were undetectable in brain and skeletal muscle of Carns1(−/−) mice (Fig. 2, *A* and *B*). Similar levels of the dipeptides were present in Carns1(+/+) and Carns1(+/−) mice (Fig. 2*C*). This indicates that carnosine synthesis is not limited by Carns1 expression and is in line with previous observations suggesting that β-alanine availability limits carnosine synthesis *in vivo*, at least in humans and mice (27, 28). Absence of carnosine in the OE was further confirmed by immunofluorescence using a carnosine-specific antibody (Fig. 2*D*). Loss of carnosine-like immunoreactivity in Carns1(−/−) OE was not due to absence of ORN, as indicated by staining of olfactory marker protein (OMP) (Fig. 2*D*). This confirmed the specificity of the peptide antibody and absence of carnosine in OE of Carns1(−/−) mice. These mice had normal body weight, did not show any obvious abnormal behavior, and had an unaltered survival rate (see the Kaplan–Meier survival curve in Fig. 1*F*). Because the oldest mice were killed at 24 months, a decrease in the maximal life span in the absence of carnosine cannot be excluded at present. We further focused our analyses on the two tissues with the highest HCD concentration, skeletal muscle and the primary olfactory system.

Absence of carnosine and anserine does not affect excitation-contraction coupling in skeletal muscle

Muscle strength measurements of 3- and 18-month-old male mice using the grip strength test showed an age-dependent decline but no significant effect of the genotype (Fig. 3*A*). Mean muscle weight and length were normal in Carns1(−/−) at 6–8 months of age (Fig. 3, *B* and *C*), although weight and length of the extensor digitorum longus (EDL) muscle (but not soleus (SOL) muscle) showed a higher variance (weight: p = 0.0012 (F-test), length: p = 0.0176 (F-test)). The reason for this difference is unclear. Histological analyses of skeletal muscle did not reveal obvious differences between genotypes with respect to fiber diameter or the number and localization of nuclei (data not shown).

Contractile properties of skeletal muscles were examined using the EDL and SOL muscles isolated from 6–8-month-old mice. No significant shift of the relationship between stimulation frequency and relative force was observed for EDL muscles from Carns1(−/−) mice and WT controls (Fig. 3*D*). Similar results were obtained with SOL muscle (data not shown). The fatigue index in long fatigue runs using EDL muscle was virtually identical for Carns1(−/−) and Carns1(+/+) mice (Fig. 3*E*). To examine whether carnosine and anserine contribute substantially to the buffering capacity in skeletal muscle, tetanic stimulation was repeated in the presence of cinnamate (4 mM). It inhibits lactate transport and therefore causes a stronger reduction in intracellular pH during fatigue runs and intensifies the decline in peak tetanic tension (29). We therefore expected a faster decline of force in the case of a stronger acidification in Carns1(−/−) muscle in the fatigue run. Peak tetanic tension was clearly reduced in the presence of cinnamate, as anticipated (Fig. 3*E*). However, the absence of a significant difference between genotypes, indicates that the buffering capacity of carnosine and anserine in skeletal muscle is negligible or can be efficiently substituted by other compounds.

Absence of carnosine does not impair olfactory function in young Carns1(−/−) mice but does in aging Carns1(−/−) mice

Olfaction in Carns1(−/−) mice and controls was examined in young (8 months) and old (18 months) mice using the buried food, preference, and habituation/dishabituation test (Fig. 4). Time to find a buried cookie was not significant different between genotypes in young (one-way ANOVA, $F_{(2,24)} = 0.646$, $p = 0.533$) or old mice ($F_{(2,27)} = 1.067$, $p = 0.358$) (Fig. 4*A*). In the preference test, which was only performed with 18-month-old animals, mice could discriminate between the two test odors, as indicated by the significantly longer inspection time for peanut butter (preferred odor) compared with the nonpreferred odor 2-methylbutyric acid (2-MB), irrespective of the genotype (one-tailed t test, p = 0.007 for Carns1(+/+), p = 0.025 for Carns1(+/−), p = 0.001 for Carns1(−/−)) (Fig. 4*B*). In addition, we used the habituation-dishabituation test to examine whether Carns1(−/−) mice (18 months) were able to discriminate between different odors assumed to be neutral. This experiment confirmed normal olfactory function in Carns1 (−/−) mice when compared with WT controls (Fig. 4*C*). We

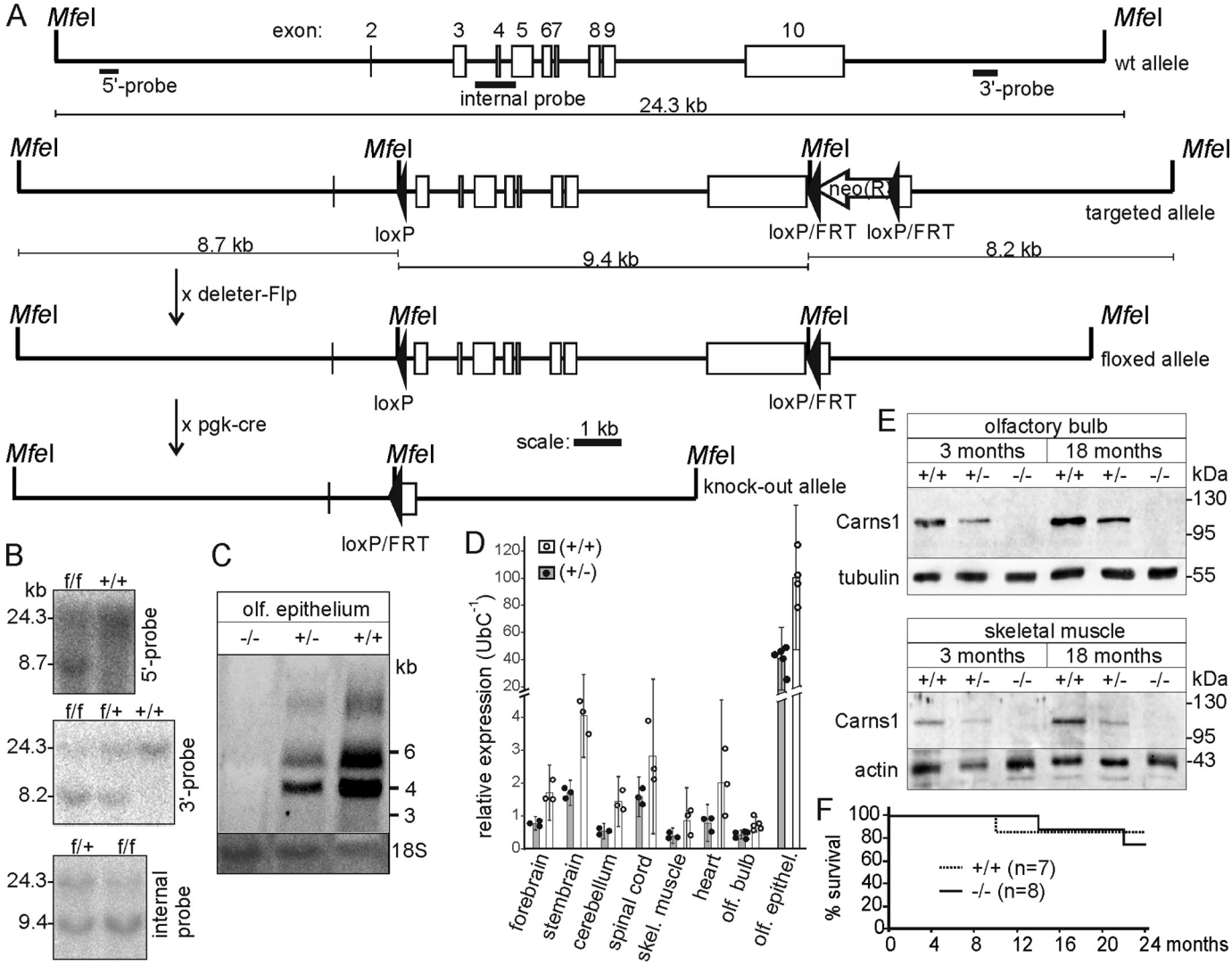

Figure 1. Generation of Carns1(−/−) mice. *A*, a loxP site was introduced upstream of exon 3, and a loxP- and FRT-flanked neomycin-resistance cassette (*neo(R)*) was inserted downstream of exon 10. Two loxP sites were linked to MfeI restriction sites to allow for homologous recombination screening by Southern blot analysis. Mice containing loxP/FRT-flanked Carns1 alleles were crossed with deleter-Flp or pgk-cre mice to generate floxed or Carns1 knockout mice. *B*, examples of Southern blotting results with selected ES clones showing WT (+/+), heterozygous (*f*/+), and homozygous floxed Carns1 (*f/f*) using the different probes indicated in *A*. The weak signal at 24.3 kb in the f/f cell line likely represents the WT allele of the feeder cells. *C*, Northern blot analysis of Carns1 expression in the OE. Note that the two separate signals around 6 and 4 kb likely belong to the same mRNA but are displaced by the 28S rRNA. *D*, quantitative real-time RT-PCR of Carns1 expression in different tissues in WT (+/+) and heterozygous Carns1(+/−) mice (Carns1 mRNA was undetectable in Carns1(−/−) mice) (n = 3–5). *E*, Western blot analysis of Carns1 in olfactory bulb and skeletal muscle (musculus gastrocnemius) using total tissue homogenates. Blots were reprobed with α-tubulin antibody to control for equal loading. *F*, Kaplan–Meier survival curve of male Carns1(−/−) (n = 8) and WT (+/+) littermates (n = 7) (mice from five litters). No significant difference by log rank test (χ^2 = 0.171; critical value = 3.84).

observed, however, that 30% of the Carns1(−/−) mice apparently did not recognize the almond odor (*i.e.* they showed a reduced inspection time in trial 4 *versus* trial 3, whereas all control mice (WT and heterozygous) showed an increased inspection time). Therefore, to detect a minor impairment in olfactory function, sensitivity assays were performed using a modified habituation-dishabituation test (Fig. 5). At 8 months of age, identical behavioral detection thresholds were observed for Carns1(−/−) and Carns1(+/+) mice for all test substances (almond, vanilla, lemon). Old (18 months) and aged (24 months) Carns1(−/−) mice, however, exhibited a higher behavioral olfactory threshold compared with WT controls for one (almond: 10-fold increased detection threshold in old mice) or two (almond: 100-fold increased detection threshold; lemon: no detection threshold reached in aged mice) of the three compounds tested (Fig. 5). In summary, the results of the olfactory tests suggest that carnosine does not affect odor perception *per se* but affects long-term functional integrity of the olfactory system.

Age-dependent decline in the number of olfactory receptor neurons in Carns1(−/−) but not in WT mice

The number of ORN in the main olfactory epithelium of endoturbinate I was determined in transverse sections of the nasal cavity obtained from 8-, 18- and 24-month-old mice (Fig. 6*A*). Sections were stained with antibodies against the ORN marker protein OMP (Fig. 6, *B–G*). Factorial ANOVA revealed

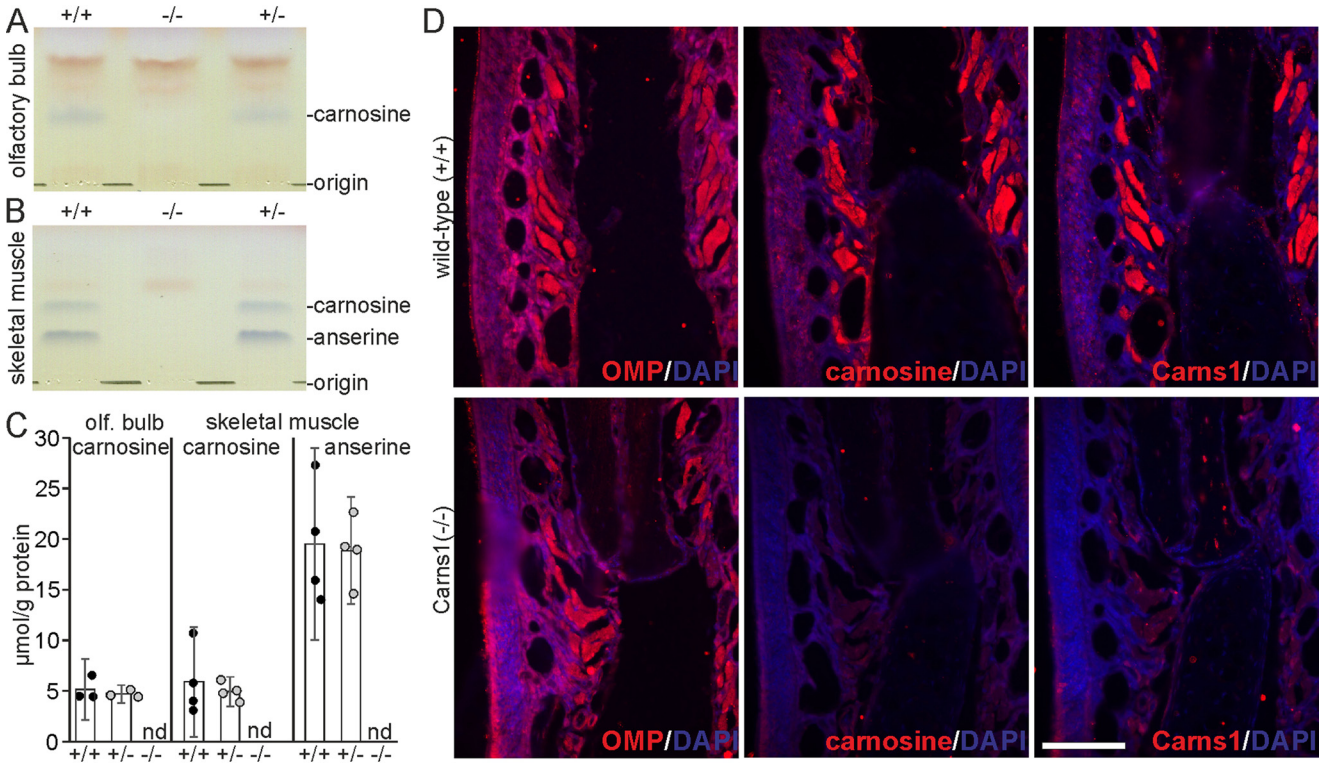

Figure 2. Carns1(−/−) mice lack detectable amounts of carnosine and anserine. *A*, HPTLC of peptide extracts from olfactory bulb of 18-month-old mice. Extracts corresponding to 0.1 mg of protein of the original tissue homogenate were separated by TLC together with increasing amounts of carnosine and anserine on separate lanes (not shown) and stained with ninhydrin. *B*, HPTLC analysis of skeletal muscle (musculus gastrocnemius) was done as described in *A*. *C*, peptides were quantified by densitometry. *Bars* and *error bars* indicate mean and 95% CI ($n = 3$ for olfactory bulb; $n = 4$ for skeletal muscle) (*nd*, not detectable). *D*, immunofluorescence staining of consecutive sections through the OE indicates the presence of Carns1 and carnosine in the OMP-positive olfactory receptor neurons in WT mice and absence of Carns1 and carnosine in Carns1(−/−) mice. Nuclei were stained with DAPI. *Scale bar*, 100 µm.

a significant effect of age ($F_{(2,18)} = 3.877$; $p = 0.039$) and genotype × age interaction ($F_{(2,18)} = 8.177$; $p = 0.003$) regarding the number of OMP-positive cells. Post hoc Newman–Keuls test indicated a significant reduction of OMP-positive cells in 24-month-old Carns1(−/−) compared with 8-month-old Carns1 (−/−) ($p = 0.003$) as well as 24-month-old controls ($p = 0.036$) (Fig. 6*H*). Thus, whereas the number of mature (OMP-positive) ORN in adult control mice did not change significantly with age, which is in agreement with previous reports (30, 31), we observed a progressive loss of mature ORN in Carns1(−/−) mice.

Apoptotic cells in the OE (determined by TUNEL assay) of 24-month-old mice were rarely detectable in both WT (in line with a previous report (32)) and Carns1(−/−) mice (Fig. 6, *I* and *J*). Moreover, these apoptotic cells were only present in the basal layer of the OE. There was no increase in the number of TUNEL-positive cells in Carns1(−/−) mice, neither in the basal nor in the apical cell layer (Fig. 6*K*). Ki67 staining did not reveal a decrease in proliferating cells in Carns1(−/−) OE, but also their number was very low in both genotypes (data not shown). Loss of ORN could potentially result from a depletion of the pool of proliferating precursor cells. However, the number of Pax6-positive basal cells in the OE was not significant different between genotypes (Fig. 6, *L–N*). Carnosine-like immunoreactivity had been observed in the rostral migratory stream, suggesting that carnosine may play a role in migration of neural precursors (33, 34). However, size of the olfactory bulb (data not shown) and the number of granule and mitral cells in the mitral cell layer were not significantly changed in Carns1(−/−) mice, suggesting no impairment of neural precursor migration into the olfactory bulb (Fig. 6, *O–Q*).

Carns1(−/−) mice show a tendency toward higher protein carbonylation, but ALEs and AGEs were not increased in the primary olfactory system

Carnosine has been shown to act as an antioxidant and to reduce protein carbonylation as well as lipoxidation and formation of ALE (4). To examine the possibility of a corresponding reversed effect in the absence of carnosine, protein-carbonyl content (using anti-DNP antibody after treating tissue sections with DNPH) and ALE protein adducts (4-hydroxy-2-nonenal (HNE) and malondialdehyde (MDA)) were determined in OE of 24-month-old mice by immunofluorescence. There were no significant changes in Carns1(−/−) mice when compared with WT controls (Fig. 7, *A–I*). However, Western blot analysis of the OB showed higher protein-carbonyl content in Carns1 (−/−) mice (Fig. 7, *J* and *K*). Total DNP signal was significantly increased in Carns1(−/−) OB ($p = 0.008$, *t* test), which was also the case when the most prominent band at 55 kDa was quantified separately (Fig. 7*K*). Attempts to prove that this band indicates increased carbonylation of tubulin and/or vimentin were unsuccessful because DNP probing of immunoprecipitated tubulin or vimentin resulted in a significant background

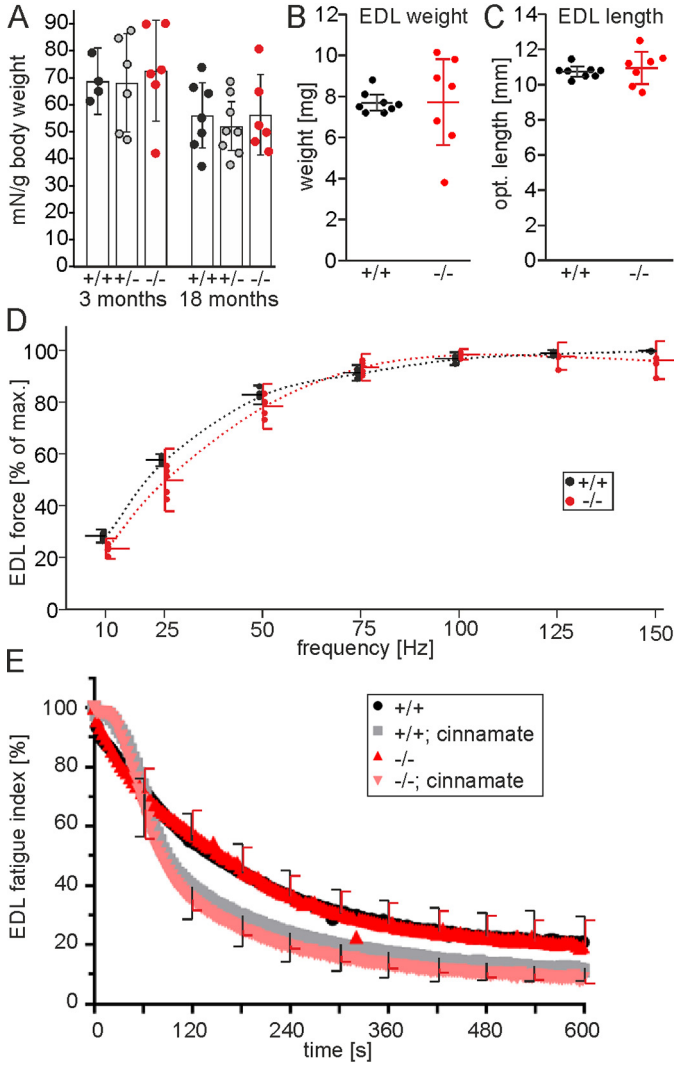

Figure 3. Muscle contractility and muscle fatigue. *A*, grip strength test of 3- and 18-month-old male Carns1(−/−), Carns1(+/−), and Carns1(+/+) mice (n = 4–8). Main effects ANOVA revealed a significant effect of age ($F_{(1,33)}$ = 11.046; p = 0.0022) but not genotype. *B–E*, EDL muscle size, contractility, and fatigue were examined with 6–8-month-old mice. Wet weight (*B*) and length of EDL muscle (*C*) were not significantly different between genotypes (n = 7–8). *D*, relationship between relative force (percentage of maximal force) and stimulation frequency for EDL muscle from WT (+/+) and Carns1(−/−) mice (n = 5). No significant difference between genotypes was observed. *E*, changes of the fatigue index in EDL muscle during long fatigue run in the absence or presence of 4 mM cinnamate (n = 4) revealed a significant effect of cinnamate treatment ($p < 0.05$; one-way ANOVA with post hoc Bonferroni test), but no significant effect of genotype. Data are shown with mean and 95% CI (in *E*, *symbols* indicate the mean, and only the upper or lower half of the 95% CI is shown for every 60 s).

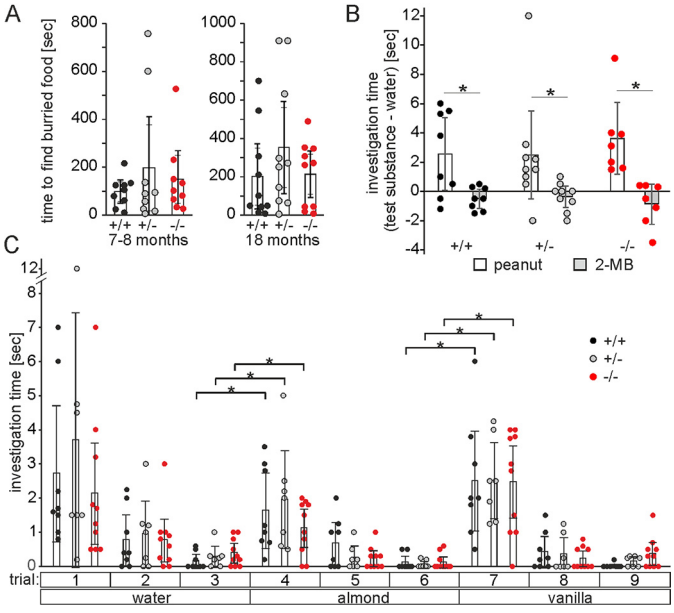

Figure 4. Olfactory function test. *A*, buried food test was performed with young (7–8 months) and old (18 months) WT (+/+), heterozygous (+/−), and homozygous Carns1(−/−) mice. The time needed to find a buried cookie was determined (cutoff time 15 min). All except two 18-month-old Carns1(+/−) mice found the cookie within 15 min. One-way ANOVA did not reveal significant differences between genotypes (n = 9 for young and n = 10 for old mice). *B*, the preference test (18-month-old mice) showed a significant difference of inspection times between the preferred (peanut butter) and the nonpreferred odor (2-MB) for all genotypes (t test; *, $p < 0.05$) (n = 8 for Carns1(+/+), n = 9 for Carns1(+/−), n = 7 for Carns1(−/−)). *C*, habituation-dishabituation tests (at 18 months) showed a significant increase in inspection time when a new odor was presented, indicating that mice of all genotypes could discriminate different odors. Values for trials 3 and 4 as well as trials 6 and 7 were tested for significant differences using Rodger's method (significant differences are indicated by *asterisks*) (n = 8 for Carns1(+/+), n = 7 for Carns1(+/−), n = 10 for Carns1(−/−)). All data are shown with mean and 95% CI. Data for male and female mice were combined.

preventing quantification of carbonyl-tubulin or vimentin (data not shown).

In contrast to this partial increase of carbonylated proteins, adducts of the lipoxidation end products HNE and MDA, examined by Western and dot blot, were not significantly increased in the carnosine-deficient OB (Fig. 7, *L–N*). Similarly, we found no evidence for increased levels of AGEs in Carns1 (−/−) OB by Western blot analysis (Fig. 7*O*). Corresponding Western and dot blot experiments shown for the OB could not be used to examine OE, because different degrees of blood contaminations (which could not be avoided) caused strong variations in the Western blotting signals that did not allow a reliable quantification (data not shown).

Discussion

Most *in vitro* studies examining the role of carnosine as an antioxidant, tumor growth inhibitor, anti-glycation, or anti-aging compound elicited a significant effect at relatively high carnosine concentrations of 10–20 mM or above (25, 35–37). Under physiological conditions, a concentration on the same order of magnitude is probably only reached in skeletal muscle and ORN (3, 4). Therefore, the possibility to draw conclusions from the above-mentioned studies on the physiological functions of HCDs is limited. Obviously, with a pK_a value of about 6.8 (for the imidazole ring), carnosine and related HCDs are efficient buffering substances at cytosolic pH. However, the HCD concentration in most tissues is too low to contribute significantly to the total buffer capacity, with the possible exception of skeletal muscle. Mannion *et al.* (38) estimated that in human skeletal muscle, carnosine accounts for about 7% of the intracellular buffer capacity, although according to other calculations, the actual contribution might be higher (39). However, whereas β-alanine supply leads to an increase in carnosine concentration that correlated with an improved exercise performance (40), there seems to be no direct evidence for alterations

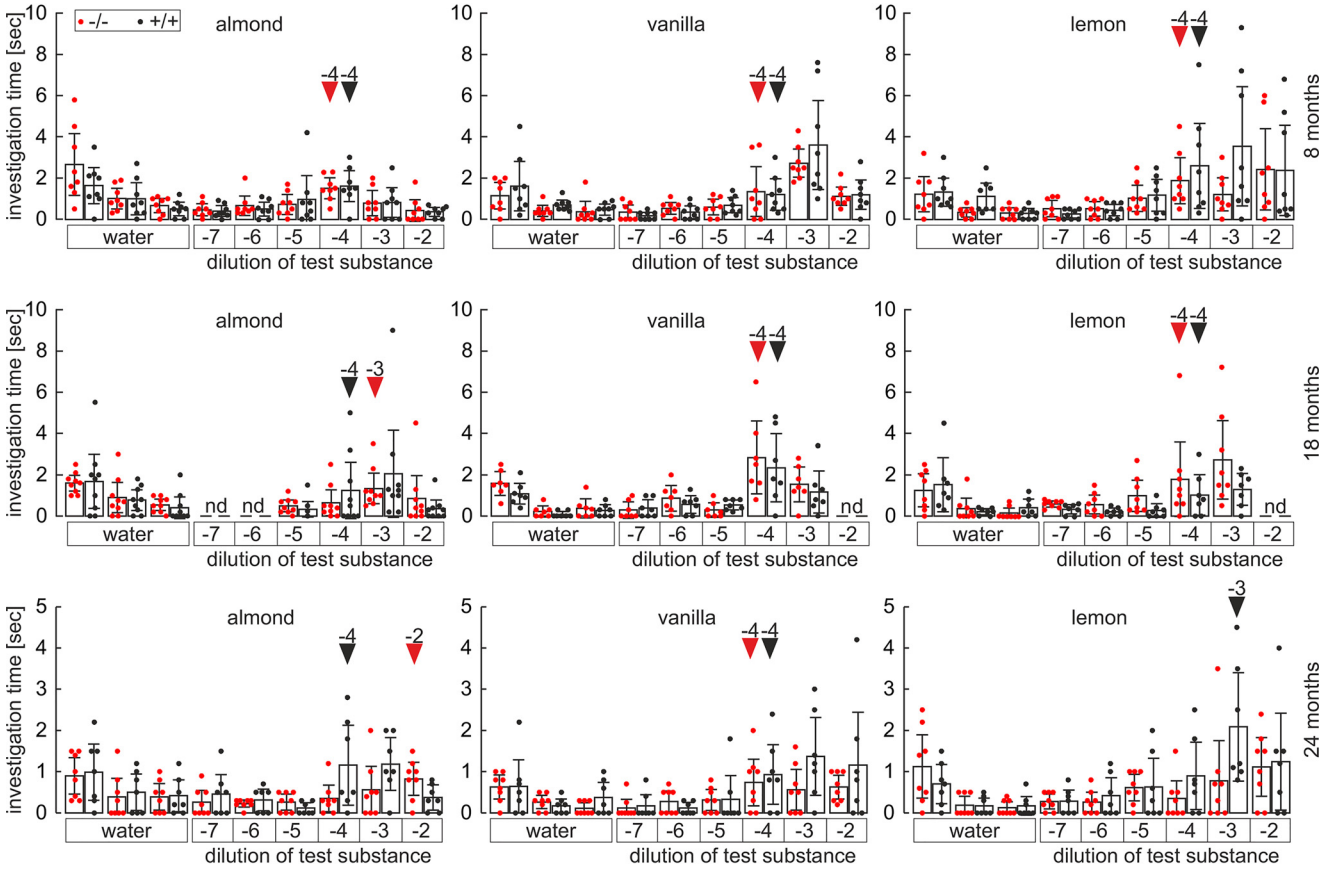

Figure 5. Olfaction sensitivity test. The behavioral detection threshold of WT (+/+) and Carns1(−/−) mice at 8, 18, and 24 months of age for different test substances (almond, vanilla, lemon; diluted 10^{-7} to 10^{-2} in water) was determined using a modified habituation-dishabituation protocol. The detection threshold (*i.e.* the test trial in which the inspection time increased significantly compared with the preceding trial for the first time) is indicated by *black* (+/+) and *red* (−/−) *arrowheads*, respectively. At 18 months, the behavioral olfactory threshold for one odor (almond) was increased 10-fold in Carns1(−/−) mice compared with WT controls (+/+). Detection of two odors (almond and lemon) was impaired in 24-month-old Carns1(−/−) mice (100-fold increased detection threshold for almond). The behavioral detection threshold for lemon odor was not reached in the case of 24-month-old Carns1(−/−) mice; therefore, no red arrowhead is shown (apparently, there is a trend toward longer inspection time). Data are shown with mean and 95% CI (8 months, $n = 8$; 18 months, $n = 7$–9; 24 months, $n = 8$ (−/−), $n = 7$ (+/+)). Data from male and female mice were combined. *nd*, not done.

in intracellular pH in post-exercise muscle after β-alanine supplementation (39). In line with this, we found that absence of HCDs did not accelerate muscle fatigue under conditions that cause a faster acidification. In principle, because carnosine/anserine are absent from Carns1(−/−) mice throughout postnatal development, loss of the HCD buffer could have been compensated by "up-regulation" of other buffers. An inducible Carns1 knockout or feeding Carns1(−/−) mice carnosine (or β-alanine) during postnatal development could be a way in future experiments to address this issue. An alternative mechanism of carnosine's action in skeletal muscle is that it may act as a shuttle, facilitating calcium supply and thereby improving excitation-contraction coupling (23, 41). Accordingly, feeding mice with a high dose of β-alanine that causes a nearly 100% increase in HCDs in EDL muscle resulted in a significant leftward shift of the force-frequency relation (24). In contrast, however, we did not observe a corresponding significant shift toward higher frequencies in the force-frequency relation in Carns1(−/−) EDL or SOL muscle. Type II fibers contain larger amounts of HCD compared with type I fibers (42). Similar to other mammals, the fiber composition in SOL (>30% type I) and EDL (>90% type II) muscle differ considerably in mice (43). The absence of a significant influence of the Carns1 genotype in both muscles therefore suggests that both fiber types were unaffected by carnosine/anserine deficiency. Thus, whereas elevated levels of carnosine can improve excitation-contraction coupling, it does not seem to play an essential role in this process. However, we did not examine muscle contractility and fatigue in older animals. Similar to the situation in the olfactory system, muscle in aging Carns1(−/−) mice may also become more susceptible to protein carbonylation, which may also impair muscle function.

ORN are possibly the only neurons synthesizing carnosine (22). Carnosine has excitatory activity at mitral (and/or tufted) cells in the OB (16), and a role as neurotransmitter or neuromodulator in the primary olfactory system has been proposed (15), although some experimental data do not support this hypothesis (see Bonfanti *et al.* (22) and De Marchis *et al.* (44) for discussion). The normal olfactory behavior and sensitivity of 8-month-old Carns1(−/−) mice suggest that carnosine does not play an essential role as a (co)transmitter for primary olfactory signal processing in the primary olfactory system. Because the olfactory discrimination task depends only on short-term memory, we cannot rule out the possibility that carnosine may play a role in long-term synaptic plasticity. On the other hand, long-term plasticity in the OB has been demonstrated for

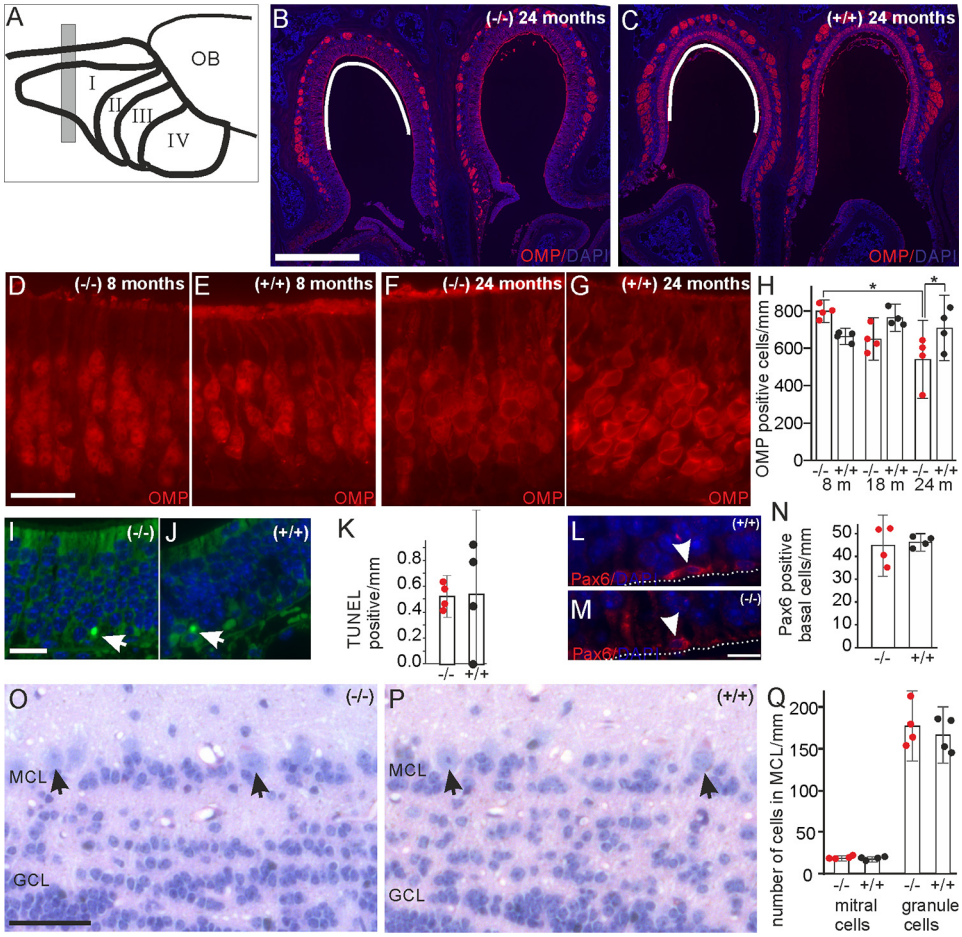

Figure 6. Age-dependent decline in the number of ORN in Carns1(−/−) mice. *A*, schematic drawing of the endoturbinates (*I–IV*) and OB to indicate the sectional plane (*gray bar*) used to collect sections (redrawn from Barrios *et al.* (76)). *B* and *C*, overview of sections stained with OMP antibody and DAPI. *White lines* indicate the areas in which OMP-positive cells were counted. *D–G*, OMP-positive cells in the dorsal part of endoturbinate I were counted in WT (+/+) and Carns1(−/−) mice at 8 (*D* and *E*), 18 (data not shown), and 24 months of age (*F* and *G*). *H*, there was an age-dependent decrease in the number of OMP-positive cells in the OE of Carns1(−/−) mice (factorial ANOVA with post hoc Newman–Keuls test; *, $p < 0.05$). *I* and *J*, apoptotic cells as determined by TUNEL assay (24-month-old mice) were rarely detectable in both genotypes, and there was no increase in their number in Carns1(−/−) mice (*K*). *L* and *M*, the number of Pax6-positive basal cells was determined in the OE of 24-month-old mice by immunostaining. No significant differences were found (*N*). *O* and *P*, the size and the number of mitral (*arrows*) and granule cells in the mitral cell layer (*MCL*) of the OB revealed no significant differences between genotypes in 24-month-old mice (*Q*). *Bars* and *error bars* indicate the mean and 95% CI ($n = 4$ per genotype and age group). *Scale bars*, 500 μm (*B*), 20 μm (*D* and *I*), 10 μm (*M*), and 50 μM (*O*).

dendro-dendritic synapses between granule and mitral cells (45), but to our knowledge not for the glomeruli-localized (carnosine-positive) synapses between ORN and mitral cells. Nevertheless, partial loss of olfactory sensitivity in aging Carns1(−/−) mice in association with a parallel loss of ORN implies that carnosine is required for long-term maintenance of the functional integrity of the OE. The temporal correlation suggests that loss of ORN is responsible for the increased olfactory behavioral threshold. Reduced sensitivity for some but not all odors tested may be explained by the fact that ORN expressing different receptor genes are lost in aging OE at different rates (46, 47). Proliferating basal cells of the OE continuously generate new ORN precursor cells that are able to replace degenerated ORN throughout life, although the turnover rate declines with age (32). The progressive loss of ORN in Carns1 (−/−) mice suggests an imbalance between formation of new immature ORN and loss of mature ORN. Although it appears likely that loss of carnosine affects survival of ORN (*i.e.* the only cells in the OE that synthesize and contain carnosine), we could not trace their loss to a higher rate of apoptosis in the ORN cell layer. It is known that the apoptosis rate of mature ORN in old OE is very low, and apoptotic cells are mainly found in the basal layer of the OE, containing less mature ORN and their precursors (32). In line with this, we found apoptotic cells only in the basal layer of the OE but not in the apical layer containing mature ORN. Possibly the increase in death rate of Carns1 (−/−) ORN was too low to allow detection of the apoptotic cells with certainty. Loss of ORN was significant only in aged mice, which would be in line with a long-lasting effect of carnosine deficiency affecting primarily long-lived ORN, which are likely more frequent in old OE, as the turnover of ORN appears to be much slower in old compared with young OE (32, 48). Because carnosine is not synthesized in the proliferating basal cells, it seems unlikely that Carns1 deficiency directly affects these cells, especially in view of the normal level of Pax6-positive precursor cells in Carns1(−/−) OE.

A property of carnosine that could potentially support survival of ORN is, of course, the general antioxidant activity that

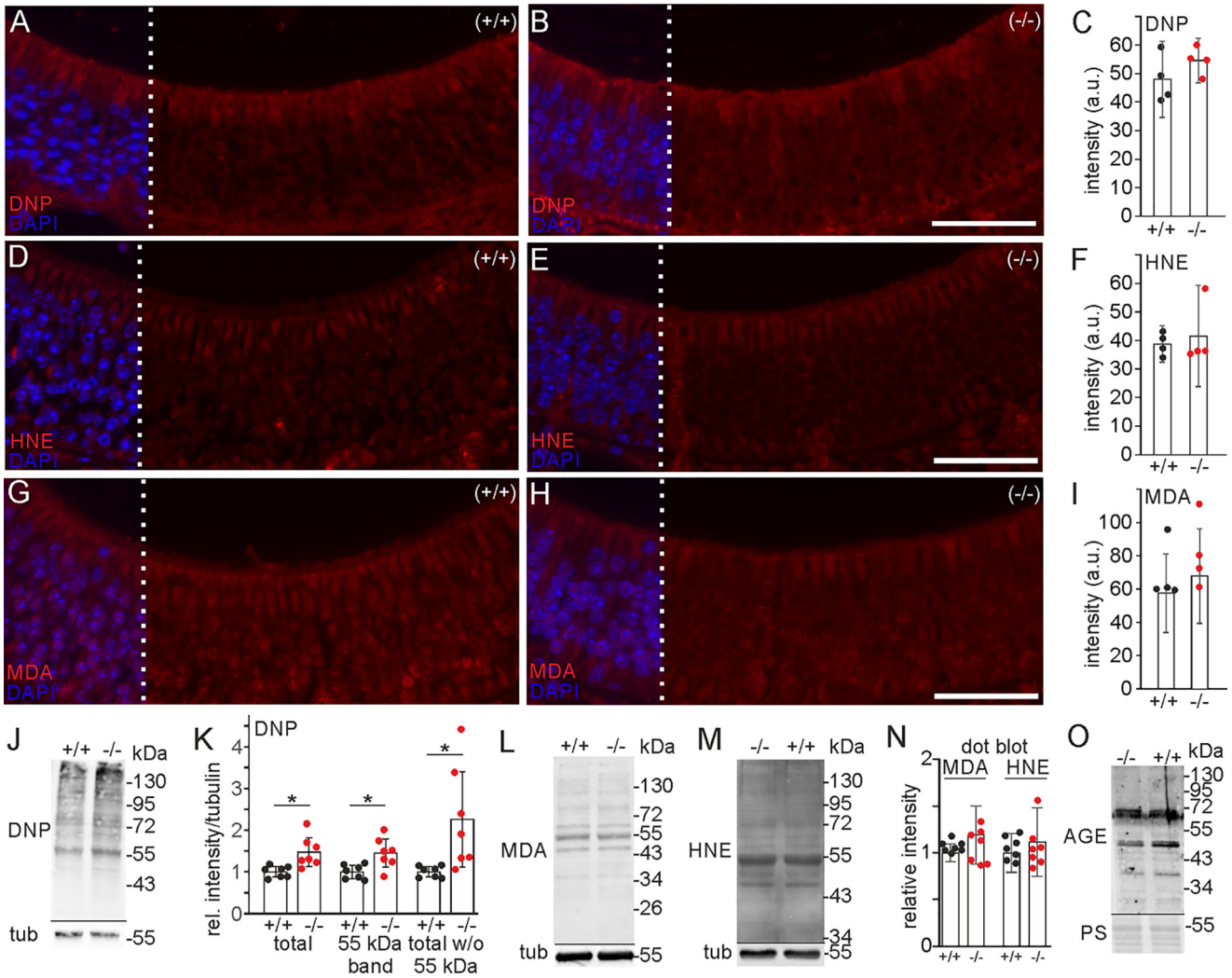

Figure 7. Partial increase of carbonyl-protein content in the OB but normal levels of lipoxidation end products in Carns1(−/−) mice. Sections of OE from 24-month-old WT (*A*) and Carns1(−/−) mice (*B*) were treated with DNPH, and DNP adducts were detected by immunofluorescence. Quantification of signals in the ORN layer did not show significant differences between genotypes (*C*). Sections from the same mice were also stained with antibodies against the ALEs HNE (*D* and *E*) and MDA (*G* and *H*). Quantification of signal intensities in the ORN layer did not show significant differences between genotypes (*F* and *I*). *Scale bars*, 50 μm. *J*, carbonyl-protein content in the OB in 22–24-month-old mice was determined by Western blotting of DNPH-treated homogenates. Blots were reprobed with α-tubulin antibody. *K*, densitometric quantification indicated significant increase in protein carbonylation in Carns1(−/−) mice (area between 130 and 43 kDa; $p = 0.008$, *t* test), DNP signal at 55 kDa ($p = 0.011$), and total DNP signal without 55 kDa band ($p = 0.020$). *L*, Western blot analysis of MDA protein adducts in OB. *M*, Western blot analysis of HNE protein adducts in OB. *N*, dot blot of MDA and HNE protein adducts in OB. *O*, Western blot analysis of AGE protein adducts in OB. To control for equal loading, membranes were stained with Ponceau S (*PS*). Data are shown with mean and 95% CI ($n = 4$ (*C*, *F*, and *I*) or $n = 7$ (*K* and *N*)).

has been demonstrated in various studies (25, 49–51), although the *in vivo* antioxidative activity of carnosine has been questioned by others (52). Protein carbonylation can disturb functionality of proteins, cause intermolecular cross-linking, and alter protein turnover (53). Besides preventing carbonylation and other oxidative damage of proteins, carnosine may also inhibit cross-linking by reacting with carbonylated proteins (54). Carbonylation of tubulin can impair its polymerization and favor depolymerization of microtubules (55, 56). Thus, it is possible that the increase of protein carbonylation in Carns1(−/−) mice may impair the functional properties of ORN axons in the OB, although further studies are necessary to solve this question.

One may presume that increased carbonyl-protein content is a direct consequence of the absence of carnosine's scavenging activity toward methylglyoxal and other carbonyls (57). However, it is also possible that Carns1 deficiency causes increased production of reactive carbonyls or impairs degradation of carbonylated proteins. The absence of carnosine may also alter gene expression as demonstrated by its effect on histone acetylation (58, 59). Determination of whether increased protein carbonylation and loss of ORN may be secondary to altered gene expression will require further studies.

We did not observe a significant increase of carbonyl-protein (or HNE and MDA adducts) in the OE. Other antioxidants are thus likely to play a more important role and/or may to a large extent compensate for the loss of carnosine, at least under non-pathological conditions. Although neurons in general contain low levels of GSH (60), ORN contain relatively large amounts of GSH (61), and ALEs like HNE are efficiently quenched by

Table 1
Oligonucleotides used in this study

Sequence	Application
Carns1-specific oligonucleotides	
AACGCTGAGACGTCAGAGAAG	5′-Probe Southern blot analysis
ACACAGAGAAACCCTGTCTCGAA	
GCCTGTGCCAGGTCTCGGGA	3′-Probe Southern blot analysis
CCCTGTGGGAGGGGCACAGA	
GATTCTGGCCCCAGGCCTGC	Internal probe Southern blot analysis
GGATGCAGCTGAGCAGTTGCG	
GTCCCAGAGAGAACAGGGCTAGACA	Genotyping PCR (219 bp (WT)/383 bp (KO))
GTCTTGGGCCAGCGAATGGGA	
TCGTGTGTGGTGTATGGGAGGCA	
TCTTTGCTCAGGAGCCGAGGACA	Genotyping PCR (348 bp (WT)/513 bp (full-length))
CACAGAAGTCCCAGGGCCAAGC	
CACACGGGATGCCCACTGAGG	
GATCTCTAGACCTTCCTATCTCTGTTGCTGG	cRNA synthesis/Northern blot analysis
GATCGTCGACCTTGGCAGGGTATAGTGGTG	
GCCAGATCTTGCTCTGCCTGGATCCACTGG	Cloning Carns1 N-terminal half in pGEX-5X-1 (restriction sites: BglII, XhoI)
CGCTCGAGTTACGTCAGTCCGTAGTCCCG	
CCGAGATCTCTGCACCTGGTGGAATCAGAC	Cloning Carns1 C-terminal half in pGEX-5X-2 (restriction sites: BglII, HindIII)
GCCAAGCTTTGCTCCTTGACCCCAGTGCT	
GCGCGGGACTACGGACTGAC	Real-time PCR
CCCTCCGGTGCTCAGTCACA	
Rps2 gene	
CTGACTCCCGACCTCTGGAAA	Real-time PCR
GAGCCTGGGTCCTCTGAACA	

GSH (see Esterbauer *et al.* (62) for a review). It remains to be determined whether carnosine deficiency may have a stronger impact under conditions of increased oxidative stress as found in various neurodegenerative diseases (63–65). This is suggested by the neuroprotective activity of carnosine in different neurodegenerative model systems (66).

Experimental procedures

Generation of Carns1(−/−) mice

A conditional Carns1-knockout allele was generated by introducing loxP sites in intron 2 and downstream of the last exon (exon 10) of the Carns1 gene using the recombineering method (67). A corresponding 129AB2.2-BAC clone was obtained from SourceBioScience (Nottigham, UK). The final targeting construct (Fig. 1*A*) was transfected by electroporation into HM-1 ES cells (68). HM-1 cells are derived from 129/Ola mice. ES cells were grown on SNLP feeder cells. Clones exhibiting homologous recombination were selected by positive/negative selection using 350 μg/ml G418 and 0.5 μg/ml ganciclovir. Genomic DNA from ES cell colony replicates in 96-well plates was isolated as described (69), digested with the restriction enzyme MfeI/MunI (Thermo Fisher Scientific, Waltham, MA, USA). Southern blots were hybridized to 5′-, 3′-, and internal probes (Fig. 1*B*), which had been labeled with [^{32}P]dCTP (Hartmann Analytic, Braunschweig, Germany) using Klenow enzyme (Thermo Fisher Scientific). Probes were generated by PCR using the primers listed in Table 1. Oligonucleotides were obtained from Eurofins Genomics (Ebersberg, Germany). Bound probes were detected using a Fujifilm Bioimager. Around 400 G418/ganciclovir-resistant colonies were screened, and the targeting frequency was 1:20. One ES clone showed homologous recombination in both alleles (*f/f* in Fig. 1*B*). This clone was used for generating chimeric mice and subsequently heterozygous (Carns1(+/floxFRT)) mice. These mice were bred with Flp deleter (70) and pgk-cre transgenic mice (71) to generate Carns1-heterozygous (Carns1(+/−)) and finally Carns1(−/−) mice. Mice used in the experiments described in this report were backcrossed with C57BL/6J mice for five generations (resulting in a genetic background of about 96% C57BL/6J). Animal experiments were approved by the local and national authorities.

Antibodies

Antibodies used in this study together with supplier information and conditions of use are summarized in Table 2. Antisera directed against murine Carns1 were generated as follows. Murine Carns1 was expressed as two fragments (cDNAs encoding amino acids 1–539 and 540–947 were subcloned into pGEX-5X-1 and pGEX-5X-2, respectively) as GSH-S-transferase fusion proteins in *Escherichia coli* BL21 (DE3). Inclusion bodies were isolated and used for immunization of rabbits and guinea pigs. Two antisera specifically recognizing Carns1 by immunofluorescence and Western blotting were obtained (see Table 2). Antisera were affinity-purified using full-length hexahistidine-tagged mouse Carns1 expressed in baculovirus-infected HighFive insect cells as described (72).

RNA isolation and Northern blot analysis

RNA was isolated from mouse tissues using TRIzol (Thermo Fisher Scientific), as described (71). Northern blot analysis of mouse tissues was done using digoxigenin-labeled RNA probes, as described (72). A fragment of mouse Carns1 cDNA (nucleotides 424–1254) was amplified by PCR, using primers shown in Table 1, and subcloned into pBluescript SK(−). Digoxigenin-labeled RNA antisense probes were synthesized using T7-RNA polymerase (Roche Diagnostics, Mannheim, Germany) and a DIG RNA Labeling Mix (Roche Diagnostics). Northern blot hybridization was done as described (73).

Table 2
Antibodies used in this study

Specificity	Host species	Supplier; order no.; lot no. (if applicable)	Application[a]	Dilution
Primary antibodies				
OMP	Goat	Wako; 544-10001; IUP1001	IF	1:200
HNE	Rabbit	Alpha Diagnostics; HNE11; 301718S31-P	WB	1:4000
HNE	Rabbit	Alpha Diagnostics; HNE11; 301718S31-P	IF	1:200
HNE	Rabbit	Alpha Diagnostics; HNE11; 301718S31-P	DB	1:20,000
MDA	Rabbit	Alpha Diagnostics; MDA11; 29111259-P	WB	1:4000
MDA	Rabbit	Alpha Diagnostics; MDA11; 29111259-P	IF	1:200
MDA	Rabbit	Alpha Diagnostics; MDA11; 29111259-P	DB	1:20,000
DNP	Rabbit	Sigma; D9656; 110M4801	WB	1:5000
DNP	Rabbit	Sigma; D9656; 110M4801	IF	1:500
AGE	Rabbit	Abcam; ab23722; GR173444	WB	1:1000
α-Tubulin	Mouse	Sigma; T5168; 39M4769V	WB	1:20,000
Carnosine	Rabbit	Abcam; ab36953; GR86343-2	IF	1:250
Carns1	Guinea pig	This paper; NA[b]; NA	IF	1:250
Carns1	Rabbit	This paper; NA; NA	WB	1:1000
Pax6	Mouse	Merck; AB2237; 2965111	IF	1:400
Secondary antibodies				
Anti-rabbit peroxidase	Goat	Dianova; 111-035-003	WB	1:20,000
Anti-mouse peroxidase	Goat	Dianova; 115-035-044	WB	1:20,000
Anti-guinea pig peroxidase	Goat	Dianova; 106-035-003	WB	1:20,000
Anti-guinea pig Cy3	Goat	Dianova; 106-165-003	IF	1:500
Anti-rabbit Cy3	Goat	Dianova; 111-165-144	IF	1:500
Anti-guinea pig Alexa Fluor 647	Goat	Invitrogen; A21450	IF	1:400
Anti-mouse Alexa Fluor-546	Goat	Invitrogen; A11018	IF	1:800
Anti-goat Cy3	Donkey	Dianova; 705-165-147	IF	1:800

[a] Application: WB, Western blotting; IF, immunofluorescence; DB, dot blot.
[b] NA, not applicable.

PCR genotyping

PCR for genotyping was done using standard procedures with REDTaq® ReadyMix™ PCR Reaction Mix (Sigma–Aldrich, Munich, Germany) and the oligonucleotides shown in Table 1. All oligonucleotides were ordered from Eurofins Genomics (Ebersberg, Germany).

cDNA synthesis and quantitative RT-PCR

cDNA was synthesized using superscript II reverse transcriptase (Invitrogen), following the instructions of the manufacturer, using total RNA (1–5 μg) and oligo(dT) primers. Real-time RT-PCR was done as described (73) using the primer pairs listed in Table 1. Expression levels of Carns1 were normalized to ribosomal protein S2 (Rps2) using the $2^{-\Delta Ct}$ method.

Western blot analysis

Tissues were homogenized in homogenization buffer (10 mM HEPES, 250 mM sucrose, 1 mM EDTA, pH 7.4) with freshly added protease inhibitors (2 μg/ml leupeptin, 2 μg/ml pepstatin, 100 μg/ml Pefabloc (all from Sigma–Aldrich) or HALTprotease inhibitor mixture (Thermo Fisher Scientific)). Protein concentrations were measured using the Bio-Rad DC protein assay with BSA as standard. SDS-PAGE and semi-dry Western blotting were done using the Mini-PROTEAN Tetra cell gel electrophoresis system and Trans-Blot® SD Semi-Dry Transfer Cell (both from Bio-Rad, Feldkirchen, Germany). The protein marker used was PageRuler Prestained Protein Ladder (Thermo Fisher Scientific; catalog no. 26617; lot 00395064). Antibodies and dilutions used are listed in Table 2. Bound secondary antibodies were detected using Pierce ECL Western blotting substrate (Thermo Fisher Scientific) and a CCD camera (Fusion Solo with FusionCapt Advance Solo 4 software, Vilber Lourmat, Eberhardzell, Germany). Western blot analysis of carbonylated proteins was done as described (74). Quantitative Western blot analyses were done with samples from male and female mice; however, in each independent experiment (analyzing 2–3 biological replicates per genotype), only age- and sex-matched mice were compared, and signal intensities were normalized to the mean of WT controls.

Dot blot analysis

Dot blot analysis of carbonyl-protein content and HNE and MDA adducts was done as described by Tanito *et al.* (75). Dot intensities were quantified by densitometry using the program AIDA (Elysia-raytest, Straubenhardt, Germany).

High-performance TLC (HPTLC) of peptides

Peptide extracts were prepared by homogenization tissue samples obtained from male mice in 90% methanol using an Ultra-turrax homogenizer (IKA, Staufen, Germany) (three times for 20 s on ice). After centrifugation (10,000 × *g*, 10 min, 4 °C) to remove precipitated proteins, supernatants were dried in a vacuum centrifuge and finally dissolved in 90% methanol. The 10,000 × *g* pellet containing precipitated proteins was dissolved in 1% SDS and used for protein determination using the DC protein assay (Bio-Rad) and BSA as standard. Peptide extracts corresponding to 0.1 or 0.2 mg of protein were applied to HPTLC silica gel plates (Merck, Darmstadt, Germany), together with carnosine, anserine, and amino acid standards (all from Sigma–Aldrich), and chromatograms were developed in 1-butanol/acetic acid/water (50:25:25, v/v/v). Peptides and amino acids were visualized by spraying the TLC plates with 0.2% ninhydrin dissolved in ethanol and heating at 180 °C for 2 min. Carnosine and anserine concentrations were determined by densitometry.

Carnosine synthase–deficient mouse

Histology and immunofluorescence

Histological analyses reported were done with male mice. Mice were perfused with 4% paraformaldehyde in phosphate buffer, and tissue samples were postfixed for 16–18 h at 4 °C. Decalcification of nasal bones was done with 14% EDTA (pH 7.2). Alternatively, in some experiments, treatment with 6% TCA for up to 1 week was done. Tissue samples were embedded in paraffin and cut at 2 or 4 μm using a microtome (Leica Biosystems, Wetzlar, Germany). Heat-induced epitope retrieval was done by microwave irradiation in 10 mM citrate buffer (pH 6.0). Immunofluorescence staining was done using antibodies and dilutions listed in Table 2. Nuclei were stained with 4′,6-diamidine-2′-phenylindole dihydrochloride (DAPI) (Sigma–Aldrich). Mature ORN were counted in 2-μm paraffin sections stained with antibodies directed against OMP. For each mouse analyzed, four sections (>20 μm apart) were collected from the same area of the nasal cavity containing the main olfactory epithelium of endoturbinate I (area 23 according to the mouse nasal cavity atlas published by Barrios *et al.* (76) (accessible at http://www.usc.es/anatembriol/). This was done in three age groups (8, 18, and 24 months) using four mice per age cohort and genotype. Data were analyzed by factorial ANOVA with post hoc Newman–Keuls test using the program STATISTICA 6.0 (a p value < 0.05 was considered as significant). Pax6-positive cells in OE from 24-month-old mice were counted after immunofluorescence staining with Pax6 antibody, and data were analyzed by two-tailed t test.

Detection of carbonylated proteins by immunofluorescence was done as described (77) with modifications. Briefly, after deparaffinization, sections were rinsed in PBS (10 min) and incubated in 1 mg/ml DNPH (in 1 M HCl) for 15 min. Control slides were incubated in 1 M HCl. After washing slides three times with PBS, sections were blocked in 10% normal goat serum for 1 h and incubated with rabbit anti-DNP antiserum (diluted 1:1000; Sigma–Aldrich) overnight at 4 °C. Slides were washed three times with 0.1% Nonidet P-40 in PBS and stained with anti-rabbit-Cy3 conjugate and DAPI. Signal intensities of DNP, HNE, and MDA immunofluorescence staining were quantified using ImageJ.

TUNEL assay

Apoptotic cells were detected by TUNEL assay using the ApopTag Fluorescein In Situ Apoptosis Detection Kit (Merck), following the instructions of the manufacturer. Negative controls lacked terminal deoxynucleotidyl transferase. Positive controls slides were prepared by treating samples with DNase I (10 units/ml) for 30 min at room temperature.

Isometric force measurements

Isometric force measurements were performed as described previously (78). In brief, SOL and EDL muscles from 6–8-month-old male mice were explanted and kept in bicarbonate buffered Tyrode solution containing 118 mM NaCl, 3.4 mM KCl, 0.8 mM $MgSO_4$, 1.2 mM KH_2PO_4, 11.1 mM glucose, 25 mM $NaHCO_3$, and 2.5 mM $CaCl_2$ gassed with 95% O_2 and 5% CO_2 at room temperature. Muscles were mounted between a force transducer (TR7S) and a fixed hook within the Myostation intact (all from MyoTronic, Heidelberg, Germany). Force was recorded with a Powerlab 8/30 recording system and the LabChart software 7.1 (AD Instruments). Platinum electrodes positioned perpendicular to the muscles and a Myostim stimulator (MyoTronic) were used for electrical stimulation (0.1 ms, biphasic). Muscles were prestretched to the optimal length until single electrical stimuli applied every 10 s evoked maximal force. 2-s-long tetanic stimulation was applied every 5 min with increasing frequencies from 10, 25, 50, 75, 125, and 150 Hz to determine the maximum isometric force. Fatigue protocols consisted of a 10-min-long series of 350-ms-long 100-Hz tetanic pulses every 3.7 s, and the fatigue index was calculated by normalizing all values to the maximal force. After the first fatigue protocol, muscles were incubated with 4 mM cinnamate (Sigma–Aldrich) for 20 min, and the same protocol was repeated. Directly after experiments, muscles were blotted dry on tissue paper and weighted. The cross-sectional area was determined by multiplying the weight with the density (1.06 $mg \times mm^{-3}$) divided by the optimal length determined during prestretch. Force was normalized to the cross-sectional area of the muscle.

Grip strength test

Grip strength of male mice was measured using a power meter (Sauter, Balingen, Germany) equipped with a grasping grid. The mouse was held at the base of the tail and allowed to grasp the grid with all four paws. The mouse was then gently pulled back, and the maximum force was recorded. The test was repeated during the following 2 days, and the maximal value from the three trials was used for data analysis.

Tests of olfactory function

In preliminary tests using WT mice, we did not observe significant differences between male and female mice concerning their performance in the different olfactory tests applied in this study. Therefore, data for both genders were combined, to minimize the number of animals to be bred. The different olfactory tests were performed with separate cohorts of animals, with the exception of the preference tests, in which all 18-month-old mice had been tested in the buried food test 1 day before. Testing of the different age groups (buried food and sensitivity tests) was always done with separate cohorts of animals.

Buried food test (79)—Mice were food-deprived overnight (18 h). The test cage (area: 30 × 16 cm, height: 13 cm) contained fresh bedding (2-cm filling height), and the mouse was acclimatized to the test cage for 5 min. The mouse was placed back into its home cage for 1 min, and a piece of chocolate cookie (Leibniz Minis BLACK'N WHITE, lot no. 01.01.17/6085A; Bahlsen, Hannover, Germany) was buried in one randomly chosen corner of the test area. The mouse was then placed back into the center of the test cage and allowed to inspect it for a maximal time of 15 min. Time was stopped when the mouse grabbed or started to eat the cookie (cut-off time 15 min). Data were tested for significant differences between genotypes using one-way ANOVA.

Preference test (80)—An empty cage (area: 30 × 16 cm, height: 13 cm) was used as test arena, and flavors were

presented by soaking Whatman filter paper (2 × 2 cm) with 60 μl of diluted test substance or water. Each experiment was started by acclimatizing the mouse by placing it for 5 min into the empty test cage. Filter paper pieces soaked with water and peanut butter (KG Fancy Food Handels GmbH, Hamburg, Germany) (1 g/100 ml mineral oil (Sigma–Aldrich)), respectively, were placed into the two corners of one short side of the test cage. The mouse was allowed to explore the cage for 3 min, and the times inspecting the water-soaked paper (neutral) and the peanut butter–soaked paper (preferred odor) were measured. After a 1-min brake, the test trial was repeated with water and 2-MB (Sigma–Aldrich; nonpreferred odor) placed into the corners of the opposite short side. The difference between test substance and water inspection times was calculated, and differences between peanut butter and 2-MB were tested for significance using two-tailed *t* test, separately for each genotype.

Habituation-dishabituation test (modified after Witt et al. (80) and Arbuckle et al. (81))—After acclimatization, as for the preference test (see above), a filter paper soaked in 60 μl of test substance was placed in the center of the test cage. Test substance in trials 1–3 was water, followed by almond (diluted 1:100 in water) in trials 4–6, and vanilla (diluted 1:100 in water) in trials 7–9. Total inspection times in each test trial were determined. Because variances between consecutive trials differed significantly (as determined by F-test), data were logarithmically transformed according to the formula $\log(1 + x)$. Time differences between consecutive trials 3 and 4, as well as trials 6 and 7, were tested for significance using Rodger's method, as described by Rodger and Roberts (82). This test was selected because of its high power, because a statistically significant difference was expected for control (WT) mice.

Sensitivity test—This test was performed and evaluated as described above for the habituation-dishabituation test with the following modifications. After the three test trials with water, six trials with increasing concentrations of the test substance (dilution from $1{:}10^7$ to $1{:}10^2$) were conducted. The test was done with three different substances (almond, vanilla, and lemon aroma (all from Dr. August Oetker Nahrungsmittel KG, Bielefeld, Germany)) with the same group of mice on three successive days, with the exception of almond aroma at 18 months, which was tested with a separate cohort. The behavioral olfactory threshold was determined by calculating the test trial that showed the first significant increase in inspection time compared with its preceding trial using Rodger's method (82). Although we did not perform outlier tests, data of one mouse from one experiment (18 months, Carns1(−/−), vanilla aroma) was excluded from the analysis because this mouse did not approach the test substance–soaked filter papers during the whole test session.

Statistics

Data are presented as the mean and 95% CI. Calculations were done using Excel (Microsoft, Redmond, WA, USA), STATISTICA 6.0 (Statsoft, Tulsa, OK, USA), or GraphPad Prism (GraphPad Software, San Diego, CA, USA). Data were tested for significant differences ($p < 0.05$) using ANOVA with appropriate post hoc tests or two-tailed Student's *t* test if not otherwise indicated. Correction for multiple comparisons was done according to Hochberg (83) unless otherwise stated.

Data availability

All data are contained within the article.

Acknowledgments—We thank Jürgen Schmidt for ES cell injection and his contribution to establish the Carns1 knockout mouse line, Joachim Degen for providing cre transgenic mice, and Ivonne Becker for expert technical assistance.

Author contributions—L. W.-E. data curation; L. W.-E., A. B., T. B., and M. E. formal analysis; L. W.-E., A. B., T. B., and M. E. investigation; L. W.-E., T. B., and P. S. methodology; P. S. and M. E. supervision; P. S. and M. E. writing-review and editing; M. E. conceptualization; M. E. funding acquisition; M. E. writing-original draft; M. E. project administration.

Funding and additional information—This work was supported by Deutsche Forschungsgemeinschaft Grant EC164/4-1 (to M. E.).

Conflict of interest—The authors declare that they have no conflicts of interest with the contents of this article.

Abbreviations—The abbreviations used are: HCD, histidine-containing dipeptide; OE, olfactory epithelium; OB, olfactory bulb; AGE, advanced glycation end product; ALE, advanced lipoxidation end product; ORN, olfactory receptor neuron(s); EDL, extensor digitorum longus; SOL, soleus; ANOVA, analysis of variance; 2-MB, 2-methyl butyric acid; DNP, 2,4-dinitrophenol; DNPH, 2,4-dinitrophenylhydrazine; HNE, 4-hydroxy-2-nonenal; MDA, malondialdehyde; HPTLC, high-performance TLC; DAPI, 4′,6-diamidine-2′-phenylindole dihydrochloride; CI, confidence interval; TUNEL, terminal deoxynucleotidyltransferase-mediated dUTP nick end labeling.

References

1. Gulewitsch, W. S., and Amiradžibi, S. (1900) Ueber das Carnosin, eine neue organische Base des Fleischextractes. *Ber. Dtsch. Chem. Ges.* **33,** 1902–1903 CrossRef
2. Crush, K. G. (1970) Carnosine and related substances in animal tissues. *Comp. Biochem. Physiol.* **34,** 3–30 CrossRef Medline
3. Margolis, F. L. (1974) Carnosine in the primary olfactory pathway. *Science* **184,** 909–911 CrossRef Medline
4. Boldyrev, A. A., Aldini, G., and Derave, W. (2013) Physiology and pathophysiology of carnosine. *Physiol. Rev.* **93,** 1803–1845 CrossRef Medline
5. Kamal, M. A., Jiang, H., Hu, Y., Keep, R. F., and Smith, D. E. (2009) Influence of genetic knockout of Pept2 on the *in vivo* disposition of endogenous and exogenous carnosine in wild-type and Pept2 null mice. *Am. J. Physiol. Regul. Integr. Comp. Physiol.* **296,** R986–R991 CrossRef Medline
6. Drozak, J., Veiga-da-Cunha, M., Vertommen, D., Stroobant, V., and van Schaftingen, E. (2010) Molecular identification of carnosine synthase as ATP-grasp domain-containing protein 1 (ATPGD1). *J. Biol. Chem.* **285,** 9346–9356 CrossRef Medline
7. Drozak, J., Chrobok, L., Poleszak, O., Jagielski, A. K., and Derlacz, R. (2013) Molecular identification of carnosine *N*-methyltransferase as chicken histamine *N*-methyltransferase-like protein (HNMT-like). *PLoS ONE* **8,** e64805 CrossRef Medline

8. Drozak, J., Piecuch, M., Poleszak, O., Kozlowski, P., Chrobok, L., Baelde, H. J., and de Heer, E. (2015) Protein C9orf41 homolog is anserine-producing methyltransferase. *J. Biol. Chem.* **290,** 17190–17205 CrossRef Medline
9. Lenney, J. F., George, R. P., Weiss, A. M., Kucera, C. M., Chan, P. W., and Rinzler, G. S. (1982) Human serum carnosinase, characterization, distinction from cellular carnosinase, and activation by cadmium. *Clin. Chim. Acta* **123,** 221–231 CrossRef Medline
10. Teufel, M., Saudek, V., Ledig, J. P., Bernhardt, A., Boularand, S., Carreau, A., Cairns, N. J., Carter, C., Cowley, D. J., Duverger, D., Ganzhorn, A. J., Guenet, C., Heintzelmann, B., Laucher, V., Sauvage, C., *et al.* (2003) Sequence identification and characterization of human carnosinase and a closely related non-specific dipeptidase. *J. Biol. Chem.* **278,** 6521–6531 CrossRef Medline
11. Pandya, V., Ekka, M. K., Dutta, R. K., and Kumaran, S. (2011) Mass spectrometry assay for studying kinetic properties of dipeptidases, characterization of human and yeast dipeptidases. *Anal. Biochem.* **418,** 134–142 CrossRef Medline
12. Ferriero, D., and Margolis, F. L. (1975) Denervation in the primary olfactory pathway of mice. II. Effects on carnosine and other amine compounds. *Brain Res.* **94,** 75–86 CrossRef Medline
13. Sassoè-Pognetto, M., Cantino, D., Panzanelli, P., Verdun di Cantogno, L., Giustetto, M., Margolis, F. L., De Biasi, S., and Fasolo, A. (1993) Presynaptic co-localization of carnosine and glutamate in olfactory neurones. *Neuroreport* **5,** 7–10 CrossRef Medline
14. Rochel, S., and Margolis, F. L. (1982) Carnosine release from olfactory bulb synaptosomes is calcium-dependent and depolarization-stimulated. *J. Neurochem.* **38,** 1505–1514 CrossRef Medline
15. Burd, G. D., Davis, B. J., Macrides, F., Grillo, M., and Margolis, F. L. (1982) Carnosine in primary afferents of the olfactory system: an autoradiographic and biochemical study. *J. Neurosci.* **2,** 244–255 CrossRef Medline
16. González-Estrada, M. T., and Freeman, W. J. (1980) Effects of carnosine on olfactory bulb EEG, evoked potentials and DC potentials. *Brain Res.* **202,** 373–386 CrossRef Medline
17. Harding, J. W., and O'Fallon, J. V. (1979) The subcellular distribution of carnosine, carnosine synthetase, and carnosinase in mouse olfactory tissues. *Brain Res.* **173,** 99–109 CrossRef Medline
18. Baslow, M. H. (2010) A novel key-lock mechanism for inactivating amino acid neurotransmitters during transit across extracellular space. *Amino Acids* **38,** 51–55 CrossRef Medline
19. Bauer, K., Hallermayer, K., Salnikow, J., Kleinkauf, H., and Hamprecht, B. (1982) Biosynthesis of carnosine and related peptides by glial cells in primary culture. *J. Biol. Chem.* **257,** 3593–3597 Medline
20. Hoffmann, A. M., Bakardjiev, A., and Bauer, K. (1996) Carnosine-synthesis in cultures of rat glial cells is restricted to oligodendrocytes and carnosine uptake to astrocytes. *Neurosci. Lett.* **215,** 29–32 CrossRef Medline
21. Bakardjiev, A. (1998) Carnosine and β-alanine release is stimulated by glutamatergic receptors in cultured rat oligodendrocytes. *Glia* **24,** 346–351 CrossRef
22. Bonfanti, L., Peretto, P., De Marchis, S., and Fasolo, A. (1999) Carnosine-related dipeptides in the mammalian brain. *Prog. Neurobiol.* **59,** 333–353 CrossRef Medline
23. Swietach, P., Youm, J. B., Saegusa, N., Leem, C. H., Spitzer, K. W., and Vaughan-Jones, R. D. (2013) Coupled Ca^{2+}/H^{+} transport by cytoplasmic buffers regulates local Ca^{2+} and H^{+} ion signaling. *Proc. Natl. Acad. Sci. U. S. A.* **110,** E2064–E2073 CrossRef Medline
24. Everaert, I., Stegen, S., Vanheel, B., Taes, Y., and Derave, W. (2013) Effect of β-alanine and carnosine supplementation on muscle contractility in mice. *Med. Sci. Sports Exerc.* **45,** 43–51 CrossRef Medline
25. Kohen, R., Yamamoto, Y., Cundy, K. C., and Ames, B. N. (1988) Antioxidant activity of carnosine, homocarnosine, and anserine present in muscle and brain. *Proc. Natl. Acad. Sci. U. S. A.* **85,** 3175–3179 CrossRef Medline
26. Hipkiss, A. R. (2009) On the enigma of carnosine's anti-ageing actions. *Exp. Gerontol.* **44,** 237–242 CrossRef Medline
27. Harris, R. C., Tallon, M. J., Dunnett, M., Boobis, L., Coakley, J., Kim, H. J., Fallowfield, J. L., Hill, C. A., Sale, C., and Wise, J. A. (2006) The absorption of orally supplied β-alanine and its effect on muscle carnosine synthesis in human vastus lateralis. *Amino Acids* **30,** 279–289 CrossRef Medline
28. Derave, W., Ozdemir, M. S., Harris, R. C., Pottier, A., Reyngoudt, H., Koppo, K., Wise, J. A., and Achten, E. (2007) β-Alanine supplementation augments muscle carnosine content and attenuates fatigue during repeated isokinetic contraction bouts in trained sprinters. *J. Appl. Physiol.* **103,** 1736–1743 CrossRef Medline
29. Westerblad, H., and Allen, D. G. (1992) Changes of intracellular pH due to repetitive stimulation of single fibres from mouse skeletal muscle. *J. Physiol.* **449,** 49–71 CrossRef Medline
30. Weiler, E., and Farbman, A. I. (1997) Proliferation in the rat olfactory epithelium, age-dependent changes. *J. Neurosci.* **17,** 3610–3622 CrossRef Medline
31. Breckenridge, L. J., Cameron, J., Puri, N., Reid, O., McGadey, J., and Smith, R. A. (1997) Localised degeneration occurs in aged mouse olfactory epithelium. *J. Anat.* **191,** 151–154 CrossRef Medline
32. Kondo, K., Suzukawa, K., Sakamoto, T., Watanabe, K., Kanaya, K., Ushio, M., Yamaguchi, T., Nibu, K., Kaga, K., and Yamasoba, T. (2010) Age-related changes in cell dynamics of the postnatal mouse olfactory neuroepithelium: cell proliferation, neuronal differentiation, and cell death. *J. Comp. Neurol.* **518,** 1962–1975 CrossRef Medline
33. Peretto, P., Bonfanti, L., Merighi, A., and Fasolo, A. (1998) Carnosine-like immunoreactivity in astrocytes of the glial tubes and in newly-generated cells within the tangential part of the rostral migratory stream of rodents. *Neuroscience* **85,** 527–542 CrossRef Medline
34. Curtis, M. A., Monzo, H. J., and Faull, R. L. (2009) The rostral migratory stream and olfactory system: smell, disease and slippery cells. *Prog. Brain Res.* **175,** 33–42 CrossRef Medline
35. Shao, L., Li, Q. H., and Tan, Z. (2004) L-Carnosine reduces telomere damage and shortening rate in cultured normal fibroblasts. *Biochem. Biophys. Res. Commun.* **324,** 931–936 CrossRef Medline
36. Oppermann, H., Purcz, K., Birkemeyer, C., Baran-Schmidt, R., Meixensberger, J., and Gaunitz, F. (2019) Carnosine's inhibitory effect on glioblastoma cell growth is independent of its cleavage. *Amino Acids* **51,** 761–772 CrossRef
37. Ybarra, N., and Seuntjens, J. (2019) Radio-selective effects of a natural occurring muscle-derived dipeptide in A549 and normal cell lines. *Sci. Rep.* **9,** 11513 CrossRef Medline
38. Mannion, A. F., Jakeman, P. M., Dunnett, M., Harris, R. C., and Willan, P. L. (1992) Carnosine and anserine concentrations in the quadriceps femoris muscle of healthy humans. *Eur. J. Appl. Physiol. Occup. Physiol.* **64,** 47–50 CrossRef Medline
39. Matthews, J. J., Artioli, G. G., Turner, M. D., and Sale, C. (2019) The physiological roles of carnosine and β-alanine in exercising human skeletal muscle. *Med. Sci. Sports Exerc.* **51,** 2098–2108 CrossRef Medline
40. Hobson, R. M., Saunders, B., Ball, G., Harris, R. C., and Sale, C. (2012) Effects of β-alanine supplementation on exercise performance: a meta-analysis. *Amino Acids* **43,** 25–37 CrossRef Medline
41. Blancquaert, L., Everaert, I., and Derave, W. (2015) β-Alanine supplementation, muscle carnosine and exercise performance. *Curr. Opin. Clin. Nutr. Metab. Care* **18,** 63–70 CrossRef Medline
42. Harris, R. C., Wise, J. A., Price, K. A., Kim, H. J., Kim, C. K., and Sale, C. (2012) Determinants of musclecarnosine content. *Amino Acids* **43,** 5–12 CrossRef Medline
43. Augusto, V., Padovani, C. R., and Campos, G. E. R. (2004) Skeletal muscle fiber types in C57BL6J mice. *Braz. J. Morphol. Sci.* **21,** 89–94
44. De Marchis, S., Modena, C., Peretto, P., Migheli, A., Margolis, F. L., and Fasolo, A. (2000) Carnosine-related dipeptides in neurons and glia. *Biochemistry (Mosc.)* **65,** 824–833 Medline
45. Liu, Z., Chen, Z., Shang, C., Yan, F., Shi, Y., Zhang, J., Qu, B., Han, H., Wang, Y., Li, D., Südhof, T. C., and Cao, P. (2017) IGF1-dependent synaptic plasticity of mitral cells in olfactory memory during social learning. *Neuron* **95,** 106–122 CrossRef Medline
46. Lee, A. C., Tian, H., Grosmaitre, X., and Ma, M. (2009) Expression patterns of odorant receptors and response properties of olfactory sensory neurons in aged mice. *Chem. Senses* **34,** 695–703 CrossRef Medline
47. Khan, M., Vaes, E., and Mombaerts, P. (2013) Temporal patterns of odorant receptor gene expression in adult and aged mice. *Mol. Cell. Neurosci.* **57,** 120–129 CrossRef Medline

48. Hinds, J. W., Hinds, P. L., and McNelly, N. A. (1984) An autoradiographic study of the mouse olfactory epithelium: evidence for long-lived receptors. *Anat. Rec.* **210,** 375–383 CrossRef Medline
49. Boldyrev, A. A., Dupin, A. M., Bunin, A. Y., Babizhaev, M. A., and Severin, S. E. (1987) The antioxidative properties of carnosine, a natural histidine containing dipeptide. *Biochem. Int.* **15,** 1105–1113 Medline
50. Decker, E. A., Livisay, S. A., and Zhou, S. (2000) A re-evaluation of the antioxidant activity of purified carnosine. *Biochemistry (Mosc.)* **65,** 766–770 Medline
51. Zhao, J., Posa, D. K., Kumar, V., Hoetker, D., Kumar, A., Ganesan, S., Riggs, D. W., Bhatnagar, A., Wempe, M. F., and Baba, S. P. (2019) Carnosine protects cardiac myocytes against lipid peroxidation products. *Amino Acids* **51,** 123–138 CrossRef Medline
52. Aruoma, O. I., Laughton, M. J., and Halliwell, B. (1989) Carnosine, homocarnosine and anserine: could they act as antioxidants *in vivo*? *Biochem. J.* **264,** 863–869 CrossRef Medline
53. Bizzozero, O. A. (2009) Protein carbonylation in neurodegenerative and demyelinating CNS diseases. In *Handbook of Neurochemistry and Molecular Neurobiology* (Lajtha A., Banik N., Ray S.K., eds) pp. 543–562, Springer, Boston
54. Hipkiss, A. R., Brownson, C., and Carrier, M. J. (2001) Carnosine, the anti-ageing, anti-oxidant dipeptide, may react with protein carbonyl groups. *Mech. Ageing Dev.* **122,** 1431–1445 CrossRef Medline
55. Ishiguro, K., Ando, T., Watanabe, O., and Goto, H. (2008) Specific reaction of α,β-unsaturated carbonyl compounds such as 6-shogaol with sulfhydrylgroups in tubulin leading to microtubule damage. *FEBS Lett.* **582,** 3531–3536 CrossRef Medline
56. Zhang, X., Li, Z., Zhang, Q., Chen, L., Huang, X., Zhang, Y., Liu, X., Liu, W., and Li, W. (2018) Mechanisms underlying H_2O_2-evoked carbonyl modification of cytoskeletal protein and axon injury in PC-12 cells. *Cell. Physiol. Biochem.* **48,** 1088–1098 CrossRef Medline
57. Hipkiss, A. R. (2018) Glycotoxins: dietary and metabolic origins; possible amelioration of neurotoxicity by carnosine, with special reference to Parkinson's disease. *Neurotox. Res.* **34,** 164–172 CrossRef Medline
58. Letzien, U., Oppermann, H., Meixensberger, J., and Gaunitz, F. (2014) The antineoplastic effect of carnosine is accompanied by induction of PDK4 and can be mimicked by L-histidine. *Amino Acids* **46,** 1009–1019 CrossRef Medline
59. Oppermann, H., Alvanos, A., Seidel, C., Meixensberger, J., and Gaunitz, F. (2019) Carnosine influences transcription via epigenetic regulation as demonstrated by enhanced histone acetylation of the pyruvate dehydrogenase kinase 4 promoter in glioblastoma cells. *Amino Acids* **51,** 61–71 CrossRef Medline
60. Raps, S. P., Lai, J. C., Hertz, L., and Cooper, A. J. (1989) Glutathione is present in high concentrations in cultured astrocytes but not in cultured neurons. *Brain Res.* **493,** 398–401 CrossRef
61. Kirstein, C. L., Coopersmith, R., Bridges, R. J., and Leon, M. (1991) Glutathione levels in olfactory and non-olfactory neural structures of rats. *Brain Res.* **543,** 341–346 CrossRef Medline
62. Esterbauer, H., Schaur, R. J., and Zollner, H. (1991) Chemistry and biochemistry of 4-hydroxynonenal, malonaldehyde and related aldehydes. *Free Radic. Biol. Med.* **11,** 81–128 CrossRef Medline
63. Ward, R. J., Zucca, F. A., Duyn, J. H., Crichton, R. R., and Zecca, L. (2014) The role of iron in brain ageing and neurodegenerative disorders. *Lancet Neurol.* **13,** 1045–1060 CrossRef Medline
64. Kim, G. H., Kim, J. E., Rhie, S. J., and Yoon, S. (2015) The role of oxidative stress in neurodegenerative diseases. *Exp. Neurobiol.* **24,** 325–340 CrossRef Medline
65. Bellia, F., Vecchio, G., Cuzzocrea, S., Calabrese, V., and Rizzarelli, E. (2011) Neuroprotective features of carnosine in oxidative driven diseases. *Mol. Aspects Med.* **32,** 258–266 CrossRef Medline
66. Berezhnoy, D. S., Stvolinsky, S. L., Lopachev, A. V., Devyatov, A. A., Lopacheva, O. M., Kulikova, O. I., Abaimov, D. A., and Fedorova, T. N. (2019) Carnosine as an effective neuroprotector in brain pathology and potential neuromodulator in normal conditions. *Amino Acids* **51,** 139–150 CrossRef Medline
67. Warming, S., Costantino, N., Court, D. L., Jenkins, N. A., and Copeland, N. G. (2005) Simple and highly efficient BAC recombineering using galK selection. *Nucleic Acids Res.* **33,** e36 CrossRef Medline
68. Magin, T. M., McWhir, J., and Melton, D. W. (1992) A new mouse embryonic stem cell line with good germ line contribution and gene targeting frequency. *Nucleic Acids Res.* **20,** 3795–3796 CrossRef Medline
69. Ramírez-Solis, R., Davis, A. C., and Bradley, A. (1993) Gene targeting in embryonic stem cells. *Methods Enzymol.* **225,** 855–878 CrossRef Medline
70. Lallemand, Y., Luria, V., Haffner-Krausz, R., and Lonai, P. (1998) Maternally expressed PGK-Cre transgene as a tool for early and uniform activation of the Cre site-specific recombinase. *Transgenic Res.* **7,** 105–112 Medline
71. Rodríguez, C. I., Buchholz, F., Galloway, J., Sequerra, R., Kasper, J., Ayala, R., Stewart, A. F., and Dymecki, S. M. (2000) High-efficiency deleter mice show that FLPe is an alternative to Cre-loxP. *Nat. Genet.* **25,** 139–140 CrossRef Medline
72. Saile, J. A. (2016) Untersuchungen zur Expression der murinen Carnosin-Synthase und Etablierung einer Methode zur nicht-radioaktiven Enzymaktivitaetsbestimmung. Ph.D. thesis, University of Bonn
73. Becker, I., Wang-Eckhardt, L., Yaghootfam, A., Gieselmann, V., and Eckhardt, M. (2008) Differential expression of (dihydro)ceramide synthases in mouse brain: oligodendrocyte-specific expression of CerS2/Lass2. *Histochem. Cell Biol.* **129,** 233–241 CrossRef Medline
74. Levine, R. L., Williams, J. A., Stadtman, E. R., and Shacter, E. (1994) Carbonyl assays for determination of oxidatively modified proteins. *Methods Enzymol.* **233,** 346–357 CrossRef Medline
75. Tanito, M., Brush, R. S., Elliott, M. H., Wicker, L. D., Henry, K. R., and Anderson, R. E. (2009) High levels of retinal membrane docosahexaenoic acid increase susceptibility to stress-induced degeneration. *J. Lipid Res.* **50,** 807–819 CrossRef Medline
76. Barrios, A. W., Núñez, G., Sánchez Quinteiro, P., and Salazar, I. (2014) Anatomy, histochemistry, and immunohistochemistry of the olfactory subsystems in mice. *Front. Neuroanat.* **8,** 63 CrossRef Medline
77. Dasgupta, A., Zheng, J., Perrone-Bizzozero, N. I., and Bizzozero, O. A. (2013) Increased carbonylation, protein aggregation and apoptosis in the spinal cord of mice with experimental autoimmune encephalomyelitis. *ASN Neuro* **5,** e00111 CrossRef Medline
78. Bruegmann, T., van Bremen, T., Vogt, C. C., Send, T., Fleischmann, B. K., and Sasse, P. (2015) Optogenetic control of contractile function in skeletal muscle. *Nat. Commun.* **6,** 7153 CrossRef Medline
79. Yang, M., and Crawley, J. N. (2009) Simple behavioral assessment of mouse olfaction. *Curr. Protoc. Neurosci.* Chapter 8, Unit 8.24 CrossRef Medline
80. Witt, R. M., Galligan, M. M., Despinoy, J. R., and Segal, R. (2009) Olfactory behavioral testing in the adult mouse. *J. Vis. Exp.* **23,** 949 CrossRef Medline
81. Arbuckle, E. P., Smith, G. D., Gomez, M. C., and Lugo, J. N. (2015) Testing for odor discrimination and habituation in mice. *J. Vis. Exp.* **99,** e52615 CrossRef Medline
82. Rodger, R. S., and Roberts, M. (2013) Comparison of power for multiple comparison procedures. *J. Methods Measurement Soc. Sci.* **4,** 20–47 CrossRef
83. Hochberg, Y. (1988) A sharper Bonferroni procedure for multiple tests of significance. *Biometrika* **75,** 800–802 CrossRef